STRENGTH TESTING OF REINFORCED AUTOCLAVED AERATED CONCRETE LINTELS

Nathan Stroud[1] and Jennifer Tanner[2]
[1] Architectural Engineering Student, Department of Civil /Architectural Engineering, University of Wyoming, Laramie, WY, 82070, United States, nstroud1@uwyo.edu
[2] Associate Professor, Department of Civil/Architectural Engineering, University of Wyoming, Laramie, WY, 82070, United States, TannerJ@uwyo.edu

ABSTRACT
Autoclaved Aerated Concrete (AAC) is a lightweight, cellular, precast building material capable of providing structural, thermal and fire resistance. Design provisions for AAC masonry were introduced in the 2005 masonry design code (MSJC), but these design provisions do not reference experimental testing of grouted, reinforced AAC lintels.

The hypothesis is that lightly reinforced and grouted AAC lintels, designed according to current masonry design provisions (MSJC), will be conservative. A suite of 12 lintels were tested to confirm this hypothesis. There were ten beams (lintels) to validate flexural behavior and two to validate shear behavior. Companion material tests were conducted on the AAC, grout, thin-bed mortar, and reinforcing bars to provide accurate values for evaluating the theoretical strength. Results of observed-to-calculated capacity showed that the average beam strength was 30% better than that predicted using MSJC design provisions. All data verified that AAC lintels can indeed behave in a ductile manner.

KEYWORDS: autoclaved aerated concrete, AAC, grouted lintel, beam

INTRODUCTION
Autoclaved Aerated Concrete (AAC) was originally developed in 1923, by Swedish architect Johan Axel Eriksson, as a response to the World War I energy crisis. AAC's high thermal insulation properties allowed for more efficient building materials. It was eventually picked up by a material producer in 1928 and was soon used throughout Europe. This innovative material was introduced into the U.S. market in the 1990s and more research opportunities exist. Structural design provisions for AAC shear walls are included in the current masonry design code (TMS 402) and design examples involving AAC masonry are provided in the Masonry Designer's Guide (MDG 2005). To the best of the authors' knowledge, published data on AAC masonry lintels does not exist.

Autoclaved aerated concrete (AAC) is classified as a lightweight concrete, in which air voids are entrained using an aerating agent in the mix. The raw material is then steam-cured at 160°C (320°F) and kept at a pressure of 1 kPa (150 psi) in an autoclave (Short and Kinniburgh 1961). It is used for its many structural advantages, including its fire resistance, low density, high resistance to thermal conductivity, and acoustic attenuation properties. Its lightweight characteristic also helps to ease the construction process.

Lintels are beams that horizontally span openings to accommodate doors and windows, and carry loads from walls above the opening (Figure 1a). Standard U-block construction with grouted, longitudinal steel is shown in Figure 1b).

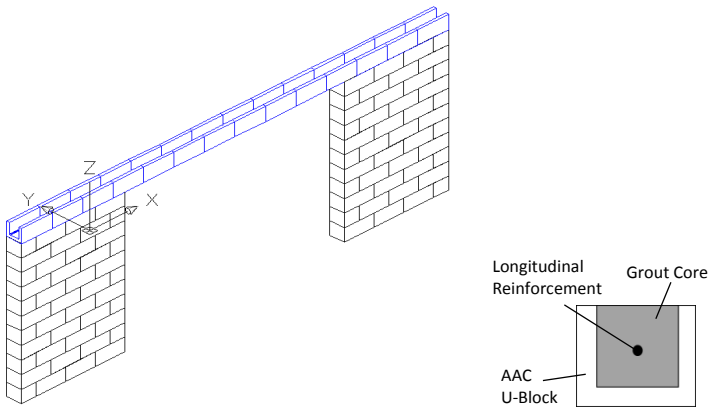

Figure 1: a) Lintel spanning opening prior to grouting b) Lintel cross-section

SPECIMEN CONSTRUCTION AND TEST SETUP

Lintel sizes were proposed that would primarily result in yielding of the steel, a ductile failure mode. With the sizes determined, 0.60 m (2 ft) long AAC pieces were joined using thin-bed mortar to create the desired length of each lintel. For each lintel length and size, reinforcing steel amounts were also selected. The steel was cut to the appropriate length, placed in the lintel, and secured with plastic rebar chairs. After waiting at least 24 hours, batches of coarse grout (ASTM C476) were mixed and used to fill the core of the lintel beams. After initial setting of the grout, the lintel beams were moved indoors into a controlled environment before testing. Curing time varied from seven to 41 days, depending on the purpose of each test and scheduling. The lintel beams were constructed and grouted in a series of six castings to spread out the testing process.

Table 1: Lintel Beam Specimens and Properties

Specimen Name	Length m	Width of AAC		Width of Core		Structural Depth		Failure mode	Steel
		m	in.	m	in.	m.	in.		
P8-6 G1	2	0.20	8	0.10	4	0.10	3.75	Flexure	2 No.3
P10-6 G1	2	0.25	10	0.13	5	0.09	3.5	Flexure	1 No.3
SP10-4 G2	1.2	0.25	10	0.13	5	0.09	3.5	Flexure	1 No.3
P10-4 G2	1.2	0.25	10	0.13	5	0.09	3.5	Flexure	1 No.3
P8-8 G3	2.4	0.20	8	0.10	4	0.10	3.75	Flexure	2 No.3
P10-8 G4	2.4	0.25	10	0.13	5	0.09	3.5	Flexure	1 No.3
P8-10 G4	3	0.20	8	0.10	4	0.10	3.75	Flexure	2 No.3
P10-10 G4	3	0.25	10	0.13	5	0.09	3.5	Flexure	2 No.3
P12-4.5 G5	1.4	0.30	12	0.15	6	0.32	12.5	Shear	2 No.4
P12-8 G5	2.4	0.30	12	0.15	6	0.11	4.5	Flexure	2 No.4
P12-8 G6	2.4	0.30	12	0.15	6	0.11	4.5	Flexure	2 No.3
P8-8 G6	3	0.2	8	0.10	4	0.32	12.5	Shear	2 No. 4

Figures 2 and 3 show a drawing of the test setup and photo of testing in progress. As shown in Figure 2, the lintel beams were subjected to four-point loading near the AAC beam center-of-span using a steel reaction frame. The frame columns are steel tubes attached to the concrete strong floor of the Kester structures lab at the University of Wyoming. A transverse loading beam pinned to the poles. Adjustable lower supports were placed on the ground. Directly under the hydraulic actuator, a semi-spherical seat was used to align the load. A series of steel rods, steel plates and thin neoprene pads were placed at the center of the beam. Initially load was applied by monitoring the force and, after yielding of the reinforcing steel, the load increments were based on measured displacements.

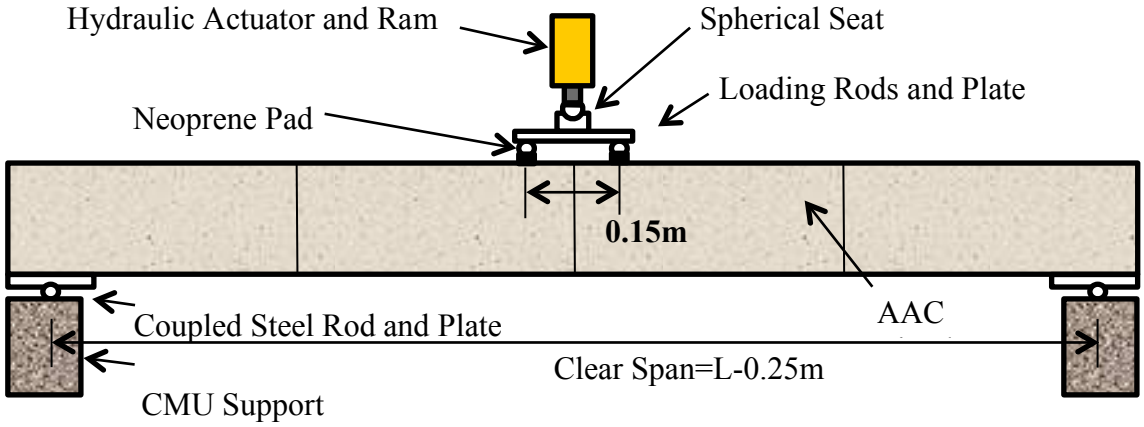

Figure 2: Flexural beam test setup

Figure 3: Specimen during testing

For each test, the applied load and corresponding displacement of the lintel specimen at each respective load point was recorded at various intervals to observe the load-versus-displacement plots. Two different, single-acting, hydraulic actuators were attached to the frame setup and used to apply a load to the beam specimens. Load was applied by hydraulic hand pump and a pressure transducer was used to monitor the load. A linear potentiometer measured the displacement of the beam during testing.

MATERIAL PROPERTIES

During each of the six grouting sessions, grout specimens were created for compression testing on the day of the beam testing. All the samples were tested on the same day as the lintel beams, to ensure that the grout had been given the same amount of time to cure and accurately represent the material property.

Grout prism molds were made by placing AAC blocks in the setup shown in Figure 3. AAC formwork replicated the water absorption that occurs in the surrounding AAC of the lintel. The grout specimens were allowed to cure for one week before being moved to a wet room to gain ultimate strength. A sulfur compound was used to cap the ends of each specimen so that the compressive force during testing would be evenly distributed to the sample regardless of surface roughness. As shown in Table 2, the grout strength ranged from 9-15 MPa (1300-2200 psi).

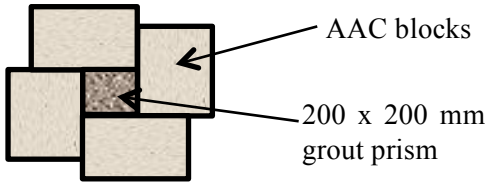

Figure 4: AAC formwork for grout prism

Select samples of AAC were taken and cut into 0.1 m x 0.1 m x 0.2 m (4 in. x 4 in. x 8 in.) specimens for compressive strength evaluation. The compressive strength of the AAC was more uniform, averaging about 2.4 MPa (355 psi). The average of these tests was used for all the theoretical calculations.

The mortar that was used to bond the AAC block segments into full length beams was a thin-set mortar made by Versabond. It is a polymer-modified, high-grade, fortified, thin-set mortar meant for application of stone, tile, walls or countertops. The mortar is easily mixed with water to

create the proper consistency, and was generously applied to both faces of the AAC at the joints. The grout mix consisted of Type 1 portland cement, masonry sand, pea gravel, and water. The pea gravel had a nominal maximum aggregate size of 9.5 millimeter (3/8 in.) diameter (ASTM C33).

Table 2: Average grout and AAC compressive strength

Grouting Session	Average Grout Prism Compressive Strength		Age at test date (days)	AAC Prism	Average AAC Prism Compressive Strength	
	MPa	psi			MPa	psi
1*	9.7	1408	7	P8-6 G1	2.9	417
2	14.2	2066	27	P10-6 G1	1.9	281
3	14.8	2147	20	P10-4 G2	2.4	354
4	9.8	1418	41	P8-8 G3	2.5	367
5	11.0	1593	28	-	-	-
6**	8.7	1266	28	-	-	-
Average	**12.5**	**1806**		**Average**	**2.4**	**355**
St. Deviation	2.45	356		**St. Deviation**	0.39	56

*Excluded from average because of shorter curing duration.
**Excluded from average because grout was not thoroughly mixed.

Both 10 mm (No. 3) and 13 mm (No. 4) reinforcing bars were used as shown in Table 1. No. 4 bars were Grade 60 ksi (MPa). All No. 3 reinforcing bars were Grade 50 and cast in the same heat; this means the yield strength exceeded 345 MPa (50 ksi). Tested yield strengths of the No. 3 bars ranged from 345-380 MPa (50 to 55 ksi) and ultimate strength was 450 MPa (70 ksi).

TEST RESULTS

Flexural tests performed on the wide variety of AAC lintel specimens described herein provided data from which conclusions about the behavior of grouted, reinforced, AAC lintels can be drawn. Figures 5 and 6 show the force-displacement behavior of the 1.2, 2, 2.4 and 3 m long beams (4, 6, 8 and 10 ft). The first two lintels were replicates and the force-displacement curve follows the same trend (Figure 5a). Different maximum loads were reached in the 2 m long specimens because the quantity of reinforcing steel was doubled in P8-6 G1 (Figure 5b). Measured displacements ranged from 50-250 mm (2-10 in.) and the observed damage in each specimen included multiple flexural cracks. Figure 6a highlights the effect of changing reinforcement in a beam. Little difference is observed in beams with widths of 0.1 and 0.13 m (8 and 10 in.) as shown in Figure 6b. Distributed flexural cracking was observed in flexure-dominated lintels (Figure 7). Cracks continued to open in a gradual manner as load was applied.

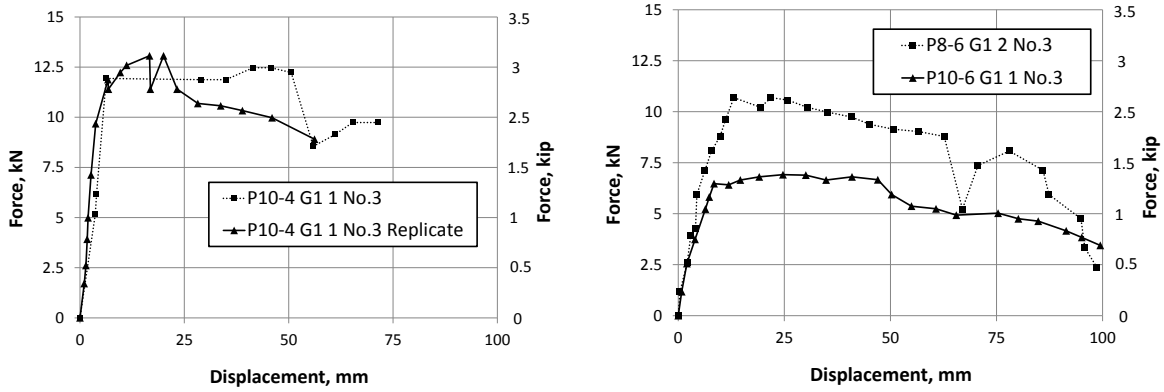

Figure 5: Measured force versus displacement curves a) 1.2 m long and b) 2 m long lintels

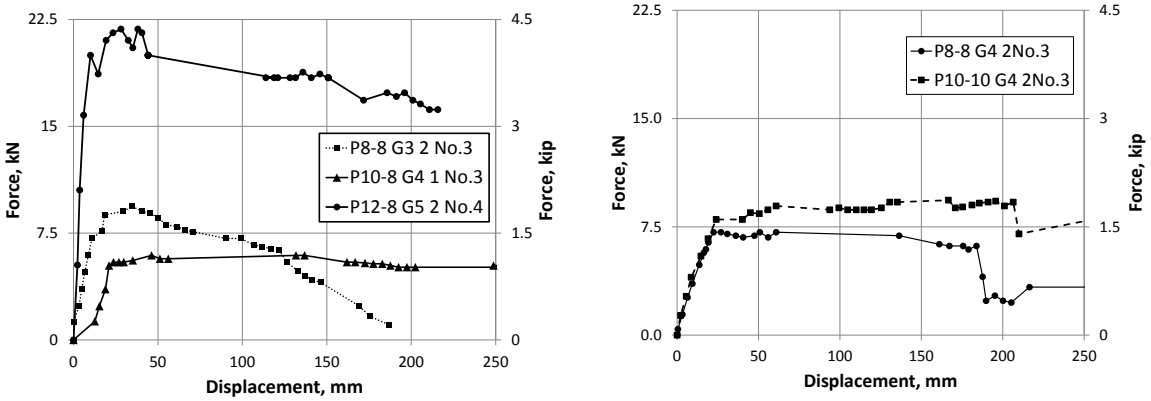

Figure 6: Measured force versus displacement curves a) 2.4 m long and b) 3 m long lintels

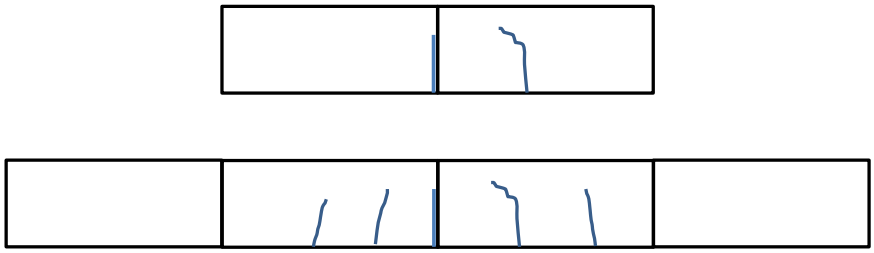

Figure 7: Observed cracking in a) 1.2 m long and b) 2.4 m long lintels

In an effort to compare data, a flexural ratio was defined (Equation 1). Results of all ten flexural specimens are presented in Figure 8, where the horizontal axis shows the flexural ratio and the yield load is plotted on the vertical axis. A linear trend is observed and the correlation coefficient (R^2) is 0.79. This value would be even closer to unity, had tensile tests been performed on each reinforcing bar used the in the project. However, this was beyond the scope of the project.

$$Flexural\ ratio = \frac{A_s d}{L} \qquad \text{Equation 1}$$

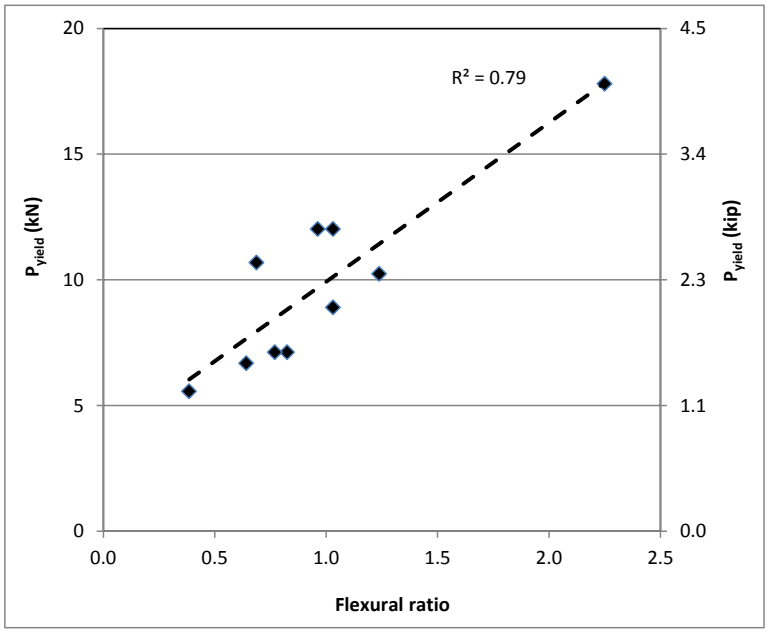

Figure 8: Normalized flexural behavior of lintel beams

Theoretical behavior was evaluated based on two conditions. The first set of calculations is the nominal flexural capacity ($f_s=f_y$ as shown in Equation 2) and the second set of calculations uses the ultimate strength ($f_s=f_u$ as shown in Equation 3) of the reinforcing bar. Ratios are presented in Figure 9 and Table 3. All lintel beams have reserve capacity when designed based on the masonry code provisions (MSJC). Calculated values of strain are reported in column 2 of Table 3. In an attempt to evaluate over-reinforced specimens, P8-6-G1, P8-10-G4 and P12-8-G5 have calculated strains less than yield. These specimens would need to be designed with less steel or additional courses to comply with the masonry code (TMS 402). The final two columns of Table 3 indicate results for the maximum load divided by the ultimate theoretical load assuming ultimate strain (f_u) is reached in the reinforcing bar. When the theoretical strain does not exced 1.5 times the yield strain, these values are not reported.

$$M_n = A_s f_y \left(d - \frac{a}{2}\right) \qquad \text{Equation 2}$$

$$M_u = A_s f_u \left(d - \frac{a}{2}\right) \qquad \text{Equation 3}$$

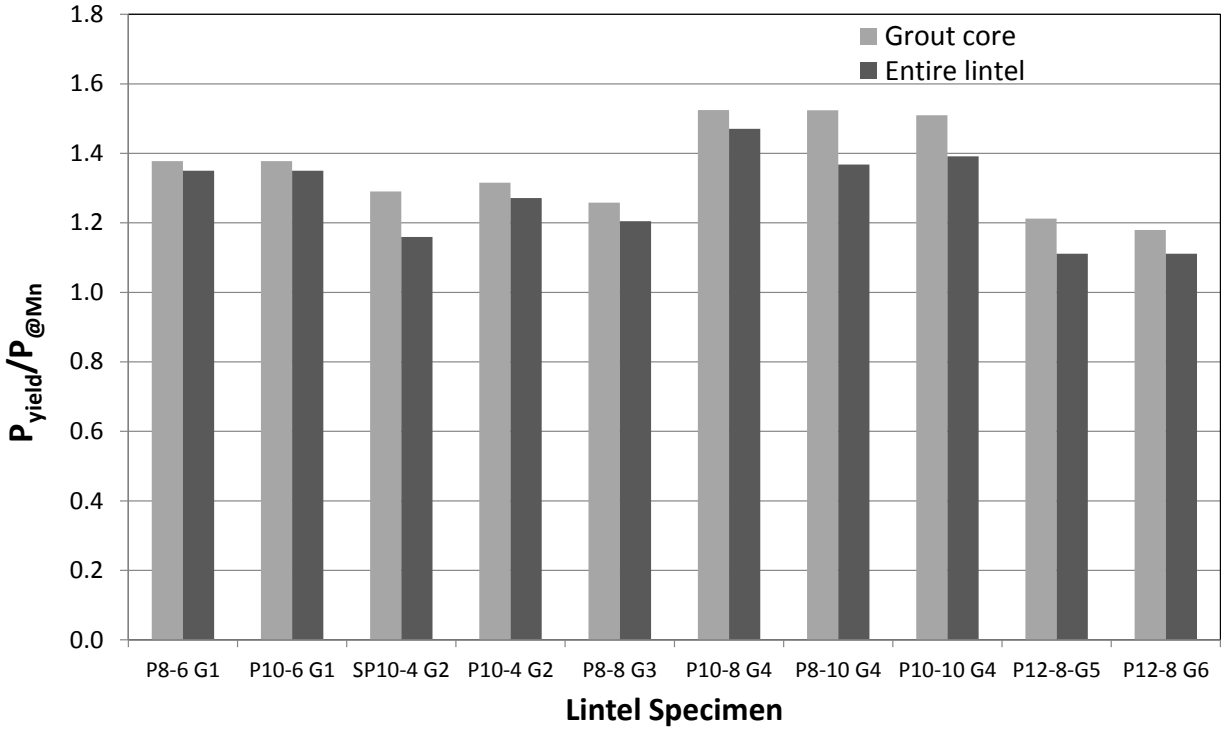

Figure 8: Ratio of P_{yield} to P at the nominal flexural capacity

Table 3: Tested versus theoretical lintel beam behavior

Specimen	Steel	Strain ratio - $\varepsilon_s/\varepsilon_y$ at M_n	$P_{yield}/P_{at\ Mn}$ ($f_s=f_y$)		P_{max}/P ($f_s=f_u$)	
			Grout core	Entire beam	Grout core	Entire beam
P8-6 G1	2 No.3	0.83	1.29	1.16	NA	NA
P10-6 G1	1 No.3	4.1	1.32	1.27	1.11	1.06
SP10-4 G2	1 No.3	6.2	1.38	1.35	1.14	1.11
P10-4 G2	1 No.3	6.2	1.38	1.35	1.19	1.13
P8-8 G3	2 No.3	1.9	1.26	1.20	1.12	1.05
P10-8 G4	1 No.3	4.1	1.52	1.47	1.32	1.26
P8-10 G4	2 No.3	0.83	1.52	1.37	NA	NA
P10-10 G4	2 No.3	1.2	1.51	1.39	NA	NA
P12-6 G5	2 No.4	NA	NA	NA	NA	NA
P12-8-G5	2 No.4	0.71	1.21	1.11	NA	NA
P12-8 G6	2 No.3	3.2	1.18	1.11	1.12	1.03
P8-8 G6	2 No.4	NA	NA	NA	NA	NA
		AVG	**1.36**	**1.28**	**1.17**	**1.11**
		St. Deviation	**0.13**	**0.13**	**0.08**	**0.08**
		COV	**9%**	**10%**	**7%**	**8%**

Because Specimens P12-6 G5 and P8-8 G6 failed in shear, they are not included in the average strength ratios for flexure. However the design shear strength can be compared to the tested strength using Equation 4, or Equation 3-23, of the masonry code (TMS 402). The ratios of observed-to-calculated strength of 1.2 and 1.3 indicate a conservative design as well. In both cases testing was halted when a brittle diagonal crack was observed in the lintel. As expected, the force-displacement behavior was linear until cracking, when the load dropped abruptly.

$$V_n = 2.25\sqrt{f_g}A_n \qquad \text{Equation 4}$$

Stiffness of each specimen was predicted theoretically using a cracked, transformed section analysis. Both the steel and AAC were transformed to the grout properties. Ratios of experimental stiffness to theoretical stiffness for each beam are presented in Table 4. Both shear specimens had a ratio of 0.35, indicating that the tested beams were more flexible than expected. Ratios of the flexural specimens ranged from 0.7 to 1.65 with an average of 1.1 and a COV of 31%. While not perfect, these calculations generally agree.

Table 4: Tested versus theoretical stiffness for each specimen

Lintel Name	Theroetical Stiffness kN/mm	Experimental Stiffness kN/mm	Theroetical Stiffness kip/in.	Experimental Stiffness kip/in.	Ratio
P8-6 G1	1.16	1.20	6.6	6.9	1.04
P10-6 G1	0.72	1.02	4.1	5.8	1.42
SP10-4 G2	2.42	1.89	13.8	10.8	0.78
P10-4 G2	2.42	1.68	13.8	9.6	0.70
P8-8 G3	0.49	0.53	2.8	3.1	1.09
P10-8 G4	0.26	0.37	1.5	2.1	1.43
P8-10 G4	0.19	0.32	1.1	1.8	1.65
P10-10 G4	0.21	0.27	1.2	1.6	1.29
P12-4.5 G5	49	18	280	100	0.36*
P12-8 G5	3.10	2.34	17.7	13.4	0.76
P12-8 G6	1.14	0.92	6.5	5.3	0.81
P8-8 G6	10.9	3.9	62	22.4	0.36*
*Excluded from average.				**Average**	**1.10**
				St. Deviation	**0.34**
				COV	**31%**

CONCLUSIONS

Flexural specimens behaved in a ductile manner based on cracking patterns and measured data. In a quantitative manner, force-displacement plots clearly indicate yielding of the longitudinal reinforcement. In addition, a linear elastic portion and yield plateau are observed. Ratios of observed to theoretical specimen behavior range from 1-1.5. The average AAC lintel performance exceeds the design capacity by a ratio of 1.28, or 28% better than theoretically determined. On average, the grouted core performs 36% better than the design capacity. The ratios of maximum tested strength to ultimate capacity (f_s=f_u) range from 1-1.3. Designs based on the masonry code are conservative.

To expand the scope of the work performed, further testing could consider the effects of additional courses of AAC blocks above the grouted portion of the beam. This action would increase the strength of beams because the depth to reinforcement is increased. Alternately, such a problem could be evaluated using finite element analysis. In addition, scaling could be performed on the results to consider longer or taller AAC lintels.

REFERENCES

1. MDG 5, 2005, “Masonry Designers’ Guide Fifth Edition”, The Masonry Society, Boulder CO.
2. Masonry Standards Joint Committee (MSJC), 2011, “Building Code Requirements for Masonry Structures”, TMS 402-11/ACI 530-11/ASCE 5-11.
3. Short, A. and Kinniburgh, W., 1961, “The Structural Use of Aerated Concrete,” The Structural Engineer, Vol. 39, pp. 1-16.
4. Nilson A.H., Darwin D., and Dolan C.W., 2010, “Design of Concrete Structures,” McGraw-Hill, Fourteenth Edition, New York, NY, p. 794.

CITED STANDARDS

1. ASTM C33, 2011, "Standard Specification for Concrete Aggregates," ASTM International, West Conshohocken, PA, www.astm.org.
2. ASTM C476, 2010, "Standard Specification for Grout for Masonry," ASTM International, West Conshohocken, PA, www.astm.org.
3. ASTM C1691, 2011, "Standard Specification for Unreinforced Autoclaved Aerated Concrete (AAC) Masonry Units," ASTM International, West Conshohocken, PA, www.astm.org.
4. ASTM C1692, 2011, "Standard Practice for Construction and Testing of Autoclaved Aerated Concrete (AAC) Masonry," ASTM International, West Conshohocken, PA, www.astm.org.
5. ASTM C1693, 2011, "Standard Specification for Autoclaved Aerated Concrete (AAC)," ASTM International, West Conshohocken, PA, www.astm.org.
6. ASTM C1694, 2009, "Standard Specification for Reinforced Autoclaved Aerated Concrete (AAC) Elements," ASTM International, West Conshohocken, PA, www.astm.org.